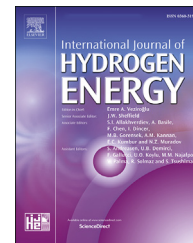




ELSEVIER

Available online at www.sciencedirect.com

ScienceDirect

journal homepage: www.elsevier.com/locate/he

Enhancement on protonation (H^+) with incorporation of flexible ethylene carbonate in CMC–PVA–30 wt % NH_4NO_3 film

M.A. Saadiah ^{a,c}, Y. Nagao ^b, A.S. Samsudin ^{c,*}

^a Department of Chemistry, Centre for Foundation Studies, International Islamic University Malaysia, 26300, Gambang, Pahang, Malaysia

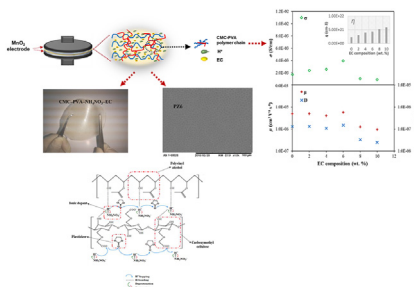
^b School of Materials Science, Japan Advanced Institute of Science and Technology, 1-1 Asahidai, Nomi, Ishikawa, 923-1292, Japan

^c Ionic Materials Team, Faculty of Industrial Sciences and Technology, Universiti Malaysia Pahang, 26300, Pahang, Malaysia

HIGHLIGHTS

- A polymer electrolytes has been prepared using CMC–PVA– NH_4NO_3 with various content of EC.
- EC substituent significantly increase the dissociation NH_4^+ – NO_3^- in polymer complexes.
- The H^+ ions contributes to the enhancement of ionic conductivity ($\sim 10^{-3}$ S/cm).
- Ionic transport via Nyquist fitting method corroborates with the trend of ionic conductivity.

GRAPHICAL ABSTRACT



ARTICLE INFO

Article history:

Received 2 November 2020

Received in revised form

8 February 2021

Accepted 21 February 2021

Available online 31 March 2021

Keywords:

Polymer blend

Physicochemical properties

ABSTRACT

In the present work, carboxymethyl cellulose (CMC)–polyvinyl alcohol (PVA)– NH_4NO_3 with the addition of ethylene carbonate (EC) based polymer blend electrolyte (PBE) was explored. The complexes of PBE with addition of EC revealed that an interaction of the $-OH$ and $-COO^-$ of the CMC–PVA blend with the dissociation of H^+ from NH_4NO_3 provides a flexibility pathway for ion hopping. The optimum ionic conductivity at room temperature was found to be 3.92×10^{-3} S/cm for the sample containing 6 wt.% EC with an increment of amorphous phase and thermal stability. Based on the Impedance-Nyquist theoretical approach, it was shown that the ionic conductivity with cation transference number ($t_{H^+} = 0.48$) of the PBE is primarily influenced by the ionic mobility as well as the ions diffusion coefficient. The findings verified that the CMC–PVA– NH_4NO_3

* Corresponding author.

E-mail address: ahmadsalihin@ump.edu.my (A.S. Samsudin).

<https://doi.org/10.1016/j.ijhydene.2021.02.187>

0360-3199/© 2021 Hydrogen Energy Publications LLC. Published by Elsevier Ltd. All rights reserved.

Conductivity
H⁺ transport

–EC possesses favorable conduction properties upon physical structural modification as a promising polymer electrolyte.

© 2021 Hydrogen Energy Publications LLC. Published by Elsevier Ltd. All rights reserved.

Introduction

The research on polymers based electrolytes system and their applications is of great technological relevance since it is regarded as a revolutionary advance for electrochemical device applications [1,2]. The physicochemical and conduction properties of polymeric materials have been well-investigated over the past decade due to their extensive range of possible applications. Among the candidates of device applications, fuel cells [3], batteries [4] and supercapacitors [5] have gained the attention of the industrial inventors and also researchers to explore the electrochemical potential of polymer electrolytes (PE). Polymer based electrolytes are regarded as solvent-free systems where its ionic conduction pathway is induced by the dissolution of ionic salts in a polymer matrix [6]. Unfortunately, low ionic conductivity exhibited by the polymer itself could be a limiting factor of their application. To date, there are numerous works and techniques in the enhancement of ionic conduction and electrochemical properties of polymer-based electrolytes. This include the addition of nano-fillers [7], plasticizer [8], blending [9] or co-polymerization [10].

The blending approach is preferred by many researchers due to its simplicity of preparation and dual function by incorporating new complexation sites between the polymer blend and ionic dopant for increased ionic conduction [11–13]. Blending polymer is the modest approach, low cost, and effective as the approach is always accompanied by a decrease in important properties including thermal and mechanical properties. The ionic conductivity of the polymer blends can be enhanced compared to single polymers due to the additional reactive sites provided by the two blended polymers [14]. Our previous work has specifically highlighted the significance of blending as an attempt to produce favorable electrochemical properties by using carboxymethyl cellulose (CMC) blended with polyvinyl alcohol (PVA) and doping with NH₄NO₃ [15,16]. The finding shows that the blended polymer CMC and PVA system had comparatively higher ionic conduction properties relative to single polymers and other polymer blends as electrolyte systems [15]. The enhancement was governed by the presence of abundant hydroxyl (-OH) and carboxylate (-COO⁻) moieties of the polymeric chain, facilitating the conduction pathway and hence boost the ionic conduction when introduced with an ionic dopant.

In continuation to the proton conduction enhancement, the addition of plasticizer is seemingly a simple approach yet, it is crucial for the polymer blend-ionic dopant complexes that contribute to a deeper understanding of the enhancement. Glycerol [17], dimethylacetamide (DMA) [18], tetra (ethylene glycol) dimethyl ether (TDE) [19], propylene carbonate (PC) [20] and ethylene carbonate (EC) [21] are known as non-volatile organic solvents and low molecular weight polymers which were reported as good plasticizers in the external method and

are commonly used as they help to improve the polymer's flexibility, extensibility and process ability. The previous work done by Chai and Isa [22] who carried out a research on CMC doped with oleic acid, managed to improve the conductivity value to 1.64×10^{-4} S/cm upon plasticizing with glycerol. Similarly, Hamsan, Aziz [23] also used glycerol as plasticizer that was added into dextran doped with NH₄NO₃ and managed to achieve higher ionic conductivity with a value of 1.13×10^{-3} S/cm. Another research performed by Shukur, Ithnin [24] used NH₄NO₃ as the ionic dopant but focusing on chitosan–starch blended biopolymer electrolyte and managed to improve the ionic conductivity to 1.02×10^{-4} S/cm when added with EC. Meanwhile, Mishra, Garg [25] also carried out polymer blending based on PMMA-PVdF that incorporated a binary mixture of EC and PC as plasticizers and obtained a conductivity value of 7.50×10^{-4} S/cm. This proves that plasticization can be considered as one of the most promising approach in the enhancement of ionic conductivity of polymer complexes as the optimization could achieve value ranges from ~10 to 4 to ~10⁻³ S/cm.

Lots of research have through in the field of polymer electrolytes in focus to their and their application, however, the investigation on ionic conduction mechanism which influences the electrochemical properties in polymer electrolytes system has not been broadly discovered due to high quantum of research on enhancement of the ionic conductivity and also the difficulty in establishing the conduction of ions especially when conduct with the dissimilar variation of ionic conductivity values. Indeed, highly ionic conductive polymer electrolyte system is anticipated towards achieving an efficient charge carrier transport and also their possible application in electrochemical devices. Charge carrier are referred to anion and cation; however, anion is usually bulky group which demonstrate lower charge transport than the cation. To address this issue, numerous number of well-documented reports on the determination of ionic transports properties have been adopted to improve the useful conduction mechanism of polymer -ionic dopant complexes. A number of comparative studies performed on a variation of transport properties assessment including FTIR deconvolution approach [8], Broadband Dielectric Response (BDR) method [26], Rice and Roth model method [27], Trukhan model [28] and Nyquist fitting method [29] that is responsible for the electrolyte's conduction properties.

FTIR deconvolution was performed to assign the free ions and contact ions from a deconvoluted peak, however, there remains a paucity of evidence on the selection of the FTIR region to be deconvoluted and also on how the two regions were assigned [30]. Bandara et al. [26], carried out a number of investigations into BDR method and found out that the method is only applicable for Nyquist plot that consist of combination semicircle and spike. In addition, the BDR method is only applicable for single relaxation mechanism in

the conduction mechanism based on dielectric behavior. Meanwhile, Rice and Roth method is only relevant for Arrhenius type behavior which yielded arguable transport properties of polymer electrolytes [31]. In the Trukhan method, shape and intensity of $\tan \delta$ peaks are very crucial in determining the transport properties parameters [32]. The presence of $\tan \delta$ peaks are due to the relaxing dipole which involved low ionic conductivity region (10^{-6} to 10^{-5} S/cm) [6]. As for the Nyquist fitting method or namely Impedance-Nyquist theoretical method (I-NT), Arof and co-worker established a method which involved data from the fitting of impedance plot solely in order to determine the transport properties [29]. This method is beneficial as it could provide deeper understanding in correlating all parameters which were evaluated from impedance spectroscopy.

In the present work, the physicochemical properties and immittance response governing the function of the plasticizer in the enhancement of ionic transport properties and conductivity of polymer blend electrolyte (PBE) was investigated. Ethylene carbonate (EC) was added to modify and boost the ionic conduction and transport properties of the PBE that emphasized on (i) the effect of the EC on the molecular properties, (ii) phase transition (iii) and ionic transport properties from Impedance Nyquist theoretical (INT) method that affects the ionic conductivity of the CMC–PVA– NH_4NO_3 –EC PBE system. This method is beneficial as it could provide deeper understanding in correlating all parameters which are evaluated from impedance spectroscopy for PBE system. Therefore, this work contributes to the coherent design of polymer based on blending system of CMC and PVA with improved properties towards the next-generation of relevant electrochemical device applications. There is no doubt that this present work is comprehensive to develop unique structure and excellent properties of the bio-based materials to serve as an electrolyte system which is significantly important in many devices.

Experimental

Materials and sample preparation

The carboxymethyl cellulose (CMC) (MW 90000; Acros Organic Co.)-polyvinyl alcohol (PVA) (MW 70000; Merck Schuchardt) blend was prepared as the host polymer and was further doped with NH_4NO_3 as ionic dopant (MW 80.04; density 0.7 g/cm³; Merck KGaA) based on the procedure reported previously [33,34]. Samples based on CMC–PVA– NH_4NO_3 –EC were prepared with varying EC contents at 2, 4, 6, 8 and 10 (w/w %) using the solution casting technique. The sample preparation and designation of the PBE are shown in Scheme 1.

Characterization of the CMC–PVA– NH_4NO_3 –EC

Attenuated total reflectance (ATR)-Fourier transform infrared (FTIR) spectroscopy

Molecular interactions of the PBE samples were characterized at ambient temperature via ATR-FTIR spectroscopy (PerkinElmer) which was outfitted with zinc selenide (ZnSe) crystal material. The spectra were recorded using the ATR mode with

a resolution of 2 cm⁻¹ and scanned within a wavenumber range of 700–4000 cm⁻¹ with the output generated in the transmittance mode in order to evaluate the effect of plasticization.

Scanning electron microscopy (SEM)

The surface morphology of the PBE was acquired by using a Tabletop Miniscope TM3030Plus (Hitachi High Technologies, Japan) where the accelerating voltage was operated at 10 kV with charge-up reduction mode and the magnification was set to 1000X.

X-ray diffraction (XRD)

XRD scans were measured qualitatively to determine the crystalline and amorphous phase. A Rigaku MiniFlex II equipped with a nickel-filtered which strikes to a metal target copper, Cu with $\lambda = 0.154$ nm generated by Cu K_α sources and tube operated at 30 kV, 15 mA was used. The 2θ angle was used to scan the PBE samples between 5° and 80° (resolution 0.1°) with 2° min⁻¹ scan rate under ambient temperature.

Differential scanning calorimetry (DSC)

DSC analysis is to investigate the phase transition properties of the PBEs such as glass transition temperature and melting temperature. The measurement was done using a TA Instruments Q500 DSC. About ~3.000 mg of PBE sample was placed and sealed in an aluminium pan. The pan was then exposed at an elevated temperature to obliterate previous thermal history, and then cooled at a linear rate before heating again at a heating rate of 10 °C min⁻¹ from 25 to 280 °C. A nitrogen flow of 50 mL min⁻¹ was applied during the measurement. The glass transition temperature (T_g) of the PBE system was obtained and analyzed using TA Universal analysis.

Electrical impedance spectroscopy (EIS)

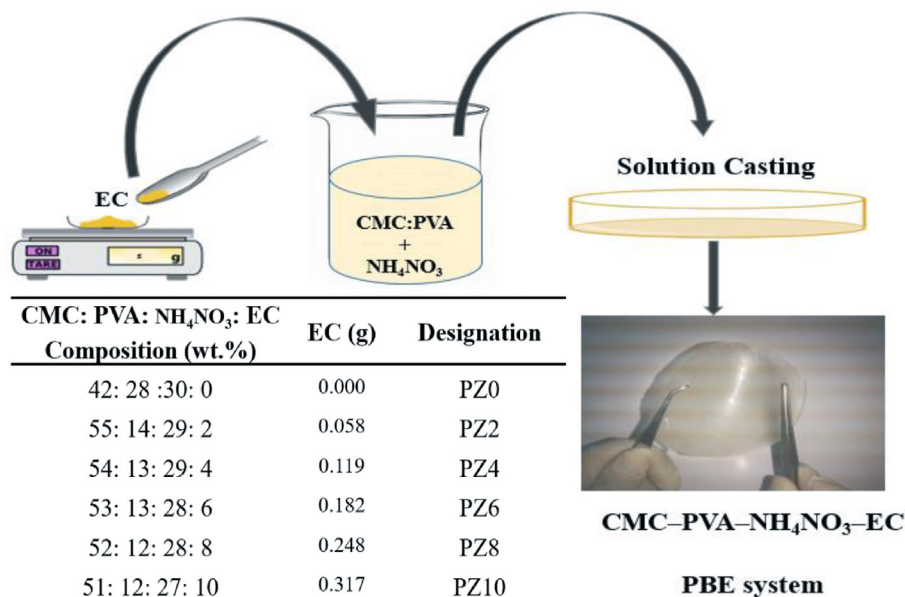
Electrical impedance spectroscopy (EIS) was carried out to determine the bulk resistance of the PBE samples using a LCR Hi-TESTER (HIOKI- 3532–50). The frequencies applied during the measurement of the ionic conductivity of the PBE were varied from 50 Hz to 1 MHz under different temperature ranges from 303 K to 353 K and at a constant voltage of 10 mV. Each PBE sample was sandwiched in between two electrodes made of stainless steel. The Nyquist plot of imaginary impedance (Z_i) versus real impedance (Z_r) enables the determination of ionic conductivity of the PBE based on the equation:

$$\sigma = \frac{1}{R_B} \times \frac{t}{A} \quad (1)$$

where t represents the PBE sample thickness, A is the cross-sectional area of contact surface and R_B is the bulk resistance.

Transference number measurement (TNM)

The transference number measurement focusing on the cation constituents (proton transference number, t_{H^+}) were performed to reveal the ionic conductivity behavior of the proton conducting PBE system. The t_{H^+} was determined by using Bruce-Vincent-Evans's technique under ambient temperature [35]. The PBE sample with the highest ionic



Scheme 1 – Schematic preparation of PBE system.

conductivity was sandwiched between two non-blocking electrodes (reversible) [36,37]. Both the anode and cathode were prepared by using manganese oxide (MnO₂), polyvinylidene fluoride (PVdF) and activated carbon (BP20) with the ratio of 77:15:8 respectively. A DC polarization technique with a fixed voltage of 0.021 V was applied to generate a plot of current as a function of time via an impedance analyzer (PGSTAT M101 with FRA32 M module Autolab) at a frequency range of 0.01 Hz–100 kHz. The t_{H^+} was calculated using the following equation:

$$t_{H^+} = \frac{I_{ss}(P - I_o R_o)}{I_o(P - I_{ss} R_{ss})} \quad (2)$$

where I_o and I_{ss} are the initial current and steady state values, respectively, P is the applied voltage, R_o and R_{ss} are the cell resistance before and after polarization, respectively [38].

Result and discussion

FTIR analysis

The interaction between the CMC–PVA host polymer with ethylene carbonate was evaluated in the absence of ammonium nitrate in order to confirm the characteristics of ethylene carbonate by using FTIR analysis. The spectra for various EC content added into un-doped CMC–PVA system is presented in Supplementary data 1. Based on the spectra, three regions were highlighted that corresponded to the C–O–C, –COO⁻ and –OH groups as they are regarded as active complexation sites [33]. Notably, the addition of EC does not demonstrate any significant changes but simply serves as wet behavior as shown at the –OH functional group. Therefore, it could be deduced that there no complexation has taken place in the system that is composed of CMC–PVA incorporated by the EC. This finding is similar to that of [24,39] who observed

no complexation between the host polymer and plasticizer added. Instead, it affects the physical appearance of the polymer electrolyte system where it is well known to give wet properties.

The interaction between EC and CMC–PVA–NH₄NO₃ was correlated to the IR-spectral changes which can be explained in detail into three different regions of wavenumbers as shown in Fig. 1. Region 1052 cm⁻¹ in Fig. 1(a) is well-known to correspond to the ether glucoside linkage –C–O–C– which is the characteristic group in the polymer of CMC polysaccharide and ethylene carbonate at a different wavenumber. As depicted in the figure, the peaks observed has shifted slightly to lower wavenumbers from PZ0 to PZ6 and further increased to higher wavenumberd with the increment of EC content. This can be associated to intermolecular attraction of van der Waals or also known as dipole-dipole force [40]. This dipole-dipole interaction creates the dipole moment at the polymer chain and hence strengthen the effective intermolecular bonds for charge transmission.

Nevertheless, in Fig. 1(b), the peak that correspond to –OH bending also experienced a shifting where the wavenumber changed from 1316 cm⁻¹ to 1329 cm⁻¹. This hydroxyl group is a polar group that is able to form hydrogen bonding (H-bonding) with another end of polarized molecules containing O or N [41]. In this case, the H₃N···H will exert an attraction towards the –OH group and form the inter-molecular H-bonding. This interaction was also sustained by the decrement in peak intensity as 2 until 10 wt % of EC was added. It is clear that the addition of EC to the PBE produced changes to the –COO⁻ at the 1581 cm⁻¹ region.

This highly nucleophilic region was expected to perform the migration of H⁺ via the Grothaus mechanism which enables the H⁺ to develop H-bonding through a hopping mechanism. This might be supported by the occurrence of stronger inter- and intra-molecular attractions known as H-bonding which happened at the conjugated π -electron system exist in

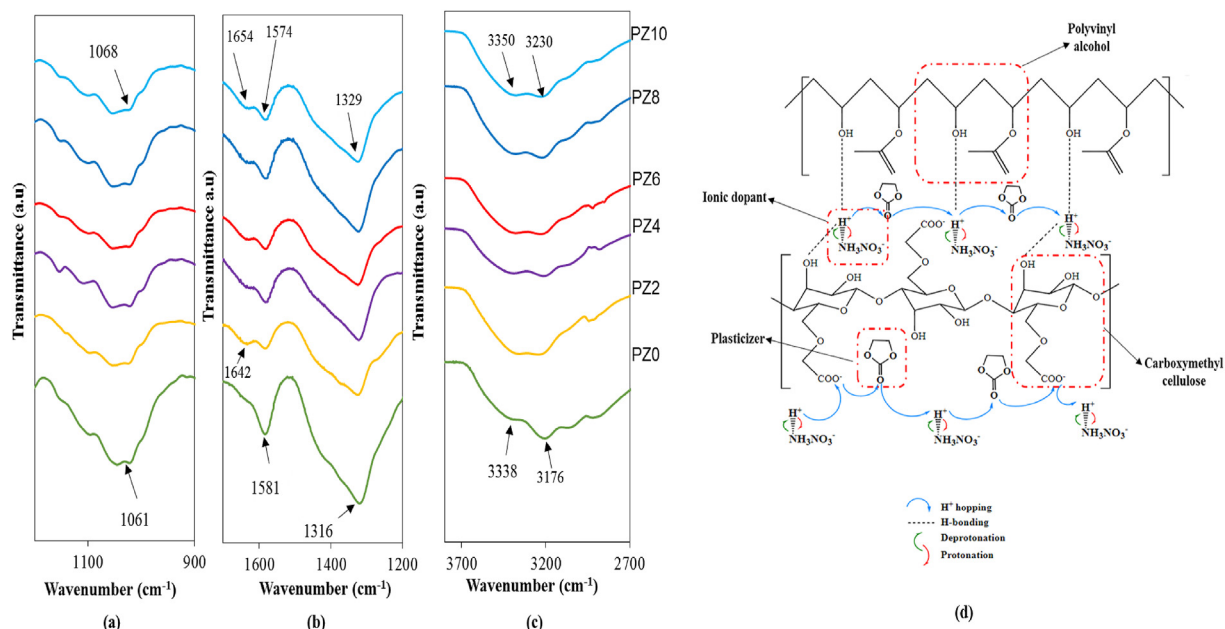


Fig. 1 – FTIR spectra for various content CMC–PVA–NH₄NO₃–EC of PBE system for selected wavenumber (a)–(c) and (d) proposed schematic diagram of H⁺ hopping mechanism in CMC–PVA–NH₄NO₃–EC.

C=O and C–O[−] of the carboxylate group respectively which can be seen through the wavenumber changes from 1581 to 1577 cm^{−1} as more EC were added. The presence of EC has assisted the quaternary ammonium nitrate to dissociate more H⁺ and building a new pathway which was weaker or temporary bonds via a faster H⁺ ion pathway and disclosed the important role of plasticizer during the complexation [42]. This can be explained by the increasing EC content causing more NH₄NO₃ to dissolve and more H⁺ to be dissociated. The enhancement of H⁺ dissociation prompted by the incorporation of EC led to more ionic coordination between H⁺ and the C–O moiety of EC to form a weak bond or flexible bonding which enable the electron conduction through the delocalized π -system [43]. These weak bonds bounded and thus, formed different pathways for H⁺ to hop into the coordinating sites (oxygen) on the CMC–PVA backbone and exert a pronounced effect in semiconducting properties. Additionally, appearance of new shoulder peak at 1642 cm^{−1} as soon as the EC was added was attributed to vibration of stretching O₂–C=O, suggesting the success of the incorporation of EC into the PBE system. The wavenumber was seen to shift to higher wavenumbers with increasing EC content. This is a reflection that this functional group is also involved in the complexation and leads to the structural improvement.

On the other hand, the region above 3000 cm^{−1} elucidates the presence of –NH and –OH stretching as depicted in Fig. 1(c). Both functional groups are significant for the occurrence of complexation. It can be noted that both wavenumber and peak intensity have changed, indicating the formation of H-bonding within this wavenumber region. This observation was found to be aligned with the work done by Hafiza and Isa [44], where these highly polarized groups have created a new pathway for the complexation to happen. Particularly, another region at 2992 cm^{−1} which belongs to the –CH group

of EC was observed in sample PZ6, suggesting the success of the plasticization to the CMC–PVA–NH₄NO₃ system. Based on the FTIR analysis, the incorporation of EC into CMC–PVA–NH₄NO₃ confirmed that the plasticization has increased the protonation by the inter-molecular interaction of weak dipole-dipole forces or strong H-bonding. This observation is expected to contribute towards the ionic conductivity enhancement through the extensive conjugated system possessed by the CMC and EC which able to conduct electron and can accommodate better ionic transport mechanism. Fig. 1(d) presents a schematic diagram that explains the interactions within the PBE incorporated with EC.

Ethylene carbonate is considered as an agent that could enhance the dissociation of the ionic dopant NH₄NO₃, resulting in more dissociation of H⁺ toward the CMC–PVA blend. In this system, it is believed that EC creates a networking with a shorter path for the H⁺ to jump and past each site more easily and freely as proposed in the schematic diagram. Based on the schematic diagram, protonation was referring to dissociation of H⁺ from the NH₄NO while the deprotonation was ascribed to H⁺ re-association and re-formed the NH₄NO₃. During the conduction mechanism, weak bonding between H⁺ and the oxygen atoms of EC was intermediately formed before hopping onto the –COO[−] of the PBE. The effective jump distance was also affected where it became shorter and caused the energy threshold to be shortened as well. Thus, this is expected to enhance the ionic conduction in the present PBE. Similar finding was reported by Hafiza and Isa [45], where they believed that the addition of a plasticizer in polymer-ionic dopant complexes would produce a weak bonding between the plasticizer and NH₄⁺, thus facilitating H⁺ hopping to another complex site. This proves that a sufficient amount of plasticizer is able to increase the flexibility of polymer-salt complexes and provide better H⁺ ion transport.

Microstructure analysis

Fig. 2 compares the surface morphology of the present system where the formation of globules were present. The images observed were consistent with our previous reports [15,16] in which the formation of indistinct globules was attributed to the non-adhesive properties of PVA. Remarkably, the PZ6 sample with 6 wt% of ethylene carbonate showed uniform dispersed globules on its surface. EC as a plasticizer is expected to enhance the structure of CMC–PVA–NH₄NO₃ which enriches the complexation and flexibility of the samples as the globule size becomes smaller. This enrichment is believed to improve the ionic conductivity of the polymer electrolyte [46]. Apparently, there is no salt agglomeration observed in all tested samples. This proves that the plasticization effect has impacted the dissociation of the NH₄NO₃ salt. This result suggests that the complexation driven by the EC addition could lead to an increase in the amorphousness where the sample is highly flexible and thus, could achieve the highest conductivity [47].

X-ray diffraction (XRD) analysis

Fig. 3 presents the result obtained from the XRD where the spectra were observed as broad with no intense peak which confirmed the amorphous phase of all of the samples incorporated with EC.

As observed in Fig. 3, the addition of EC into the CMC–PVA–NH₄NO₃ promoted for a shifting in the Bragg angle of 21.2° (PZ0) to 24.6° (PZ10). This small shifting confirmed the occurrence of complexation in the amorphous sample as

described by the FTIR analysis. Notably, sample PZ6 had the lowest peak's intensity which suggests that it is the most amorphous sample which could stimulate the segmental motion of the CMC–PVA–NH₄NO₃ polymer chain and experienced higher ionic diffusion [48]. The findings indicated that upon the addition of EC as plasticizer, the CMC–PVA–NH₄NO₃ became more flexible due to the presence of more active sites for H⁺ coordination and it also facilitated the H⁺ migration through the polymer blend-ionic dopant complexes which are in agreement with what have been reported by Liew and Ramesh [49]. The continuous ion hopping and migration along the polymer chain will subsequently increase the ionic conductivity. In addition, there were no crystalline peaks observed in the spectra, implying a complete dissolution of NH₄NO₃ and EC in the CMC–PVA host polymer which supported the observation in the FTIR analysis [50].

It was observed that the amorphousness of the CMC–PVA–NH₄NO₃ system started to decrease after further addition of 30 wt % of EC for sample PZ8 and PZ10 where the peak's intensities were increased. However, the crystalline peak was absent indicating that the sample was still amorphous with the help of the plasticizer. This was ascribed to the contribution of a higher degree protonation and thus, increased the H⁺ transport within the PBE which resulted in the amorphous phase. Higher degrees of dissociation of NH₄NO₃ is influenced by the presence of EC which could affect the conductivity.

The deconvolution approach was performed to evaluate the degree of crystallinity and amorphousness quantitatively, which has been affected by the addition of EC into the CMC–PVA–NH₄NO₃ system and presented in Supplementary

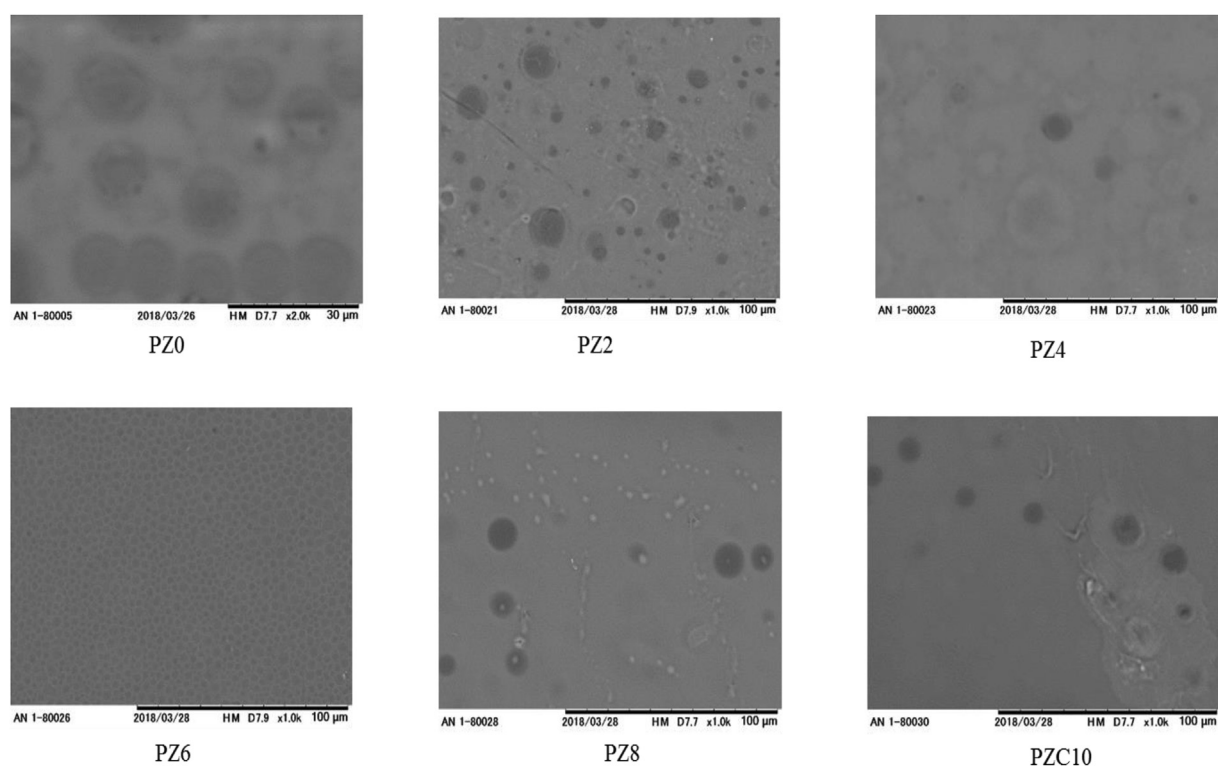


Fig. 2 – SEM images for various content CMC–PVA–NH₄NO₃–EC.

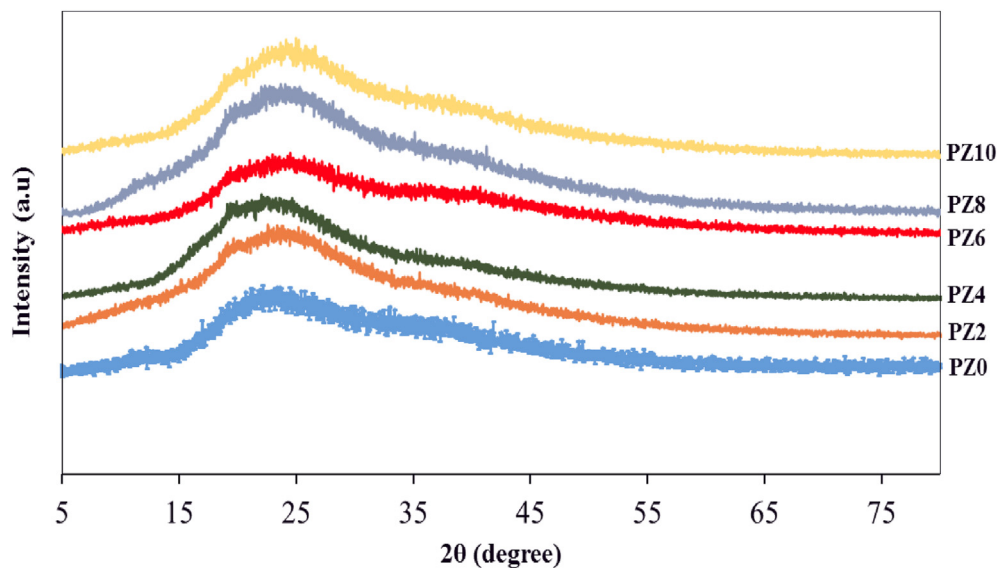


Fig. 3 – XRD spectra for various content CMC–PVA–NH₄NO₃–EC.

data 2. Based on the figure, the results showed that the amorphous peak became more apparent as more EC was added into the CMC–PVA–NH₄NO₃ and this confirmed the microstructure analysis in the previous XRD analysis. Based on the analysis, the degree of crystallinity (X_c) was determined quantitatively using following equation:

$$X_c = \frac{A_c}{A_t} \times 100 \quad (3)$$

where, X_c is the degree of crystalline in percentage, A_c is the area of crystalline region, A_t is the total area under the peak representing the area of crystalline region and amorphous area region. The calculated value of X_c revealed that the inclusion of EC managed to decrease the degree of crystallinity from 29.24% to 13.45%. The deconvolution proved that the PZ6 sample was the most amorphous. Yet, the addition of EC beyond 6 wt % gave the opposite effect on the degree of crystallinity due to the inability of the polymer blend to complex with the NH₄NO₃ which in turn causes to the ions being un-dissociated or re-associated [51].

Thermal analysis

Thermal analysis has been carried out by using differential scanning calorimetry (DSC) for the observation on the phase transition of CMC–PVA–NH₄NO₃ when incorporated with EC. Fig. 4 depicts the DSC thermogram for various contents of EC and there were two regions observed in the figure. The first region corresponds to the vaporization of water whereas the second region was ascribed to the glass transition temperature, T_g which is an important parameter for the amorphous sample. The single T_g indicates the miscibility among the constituent components which were CMC–PVA, NH₄NO₃ and EC [52]. Frequently, the T_g of polymers could be reduced by the addition of a plasticizer and hence, influence the dissociation of ionic dopant, chain stiffness, and chain flexibility [53].

It was noticed that the addition of EC into the CMC–PVA–NH₄NO₃ has reduced the T_g to a certain extent. The reduction may be attributed to the creation of transient or temporary bonding during the complexation between the CMC–PVA–NH₄NO₃ and EC as discussed earlier and also reported by Jiang, Zhang [42]. This led to the reduction of the energy barrier, thus requiring less energy for the protonation and migration of H⁺ which portrays a remarkable plasticization effect and eventually varied the glass transition properties of the plasticized CMC–PVA–NH₄NO₃ as tabulated in Fig. 4. The optimum added EC content could manipulate the T_g value and demonstrated the lowest value in the PZ6 sample.

The findings demonstrate that the phase transition of the CMC–PVA–NH₄NO₃ depends mostly on the content of EC as plasticizer. The data showed that the T_g for CMC–PVA–NH₄NO₃ added with EC was reduced from 89.91 °C (PZ2) to 84.02 °C (PZ6). This decrement of T_g is primarily due to the strong plasticizing effect which transformed the system to become highly amorphous which is aligned with the XRD discussed earlier. This feature helps in promoting the ions transport or migration through the entire polymer chain which in turn increases the ionic conductivity. This could be ascribed to a possible complexation when EC was included to the CMC–PVA–NH₄NO₃ that allows for more dissociation of the ammonium nitrate. In another perspective reported by Dixon, Ford [54], polyalkylene or cyclic carbonate such as EC will undergo chain scission or cleavage at the end chain and hence becomes more flexible, leading to lower T_g .

Apart from this, the addition of 8 wt % EC increased the T_g value slightly to 84.57 °C. The increment of T_g in PZ8 could be due to excessive amount of EC which led the formation of linkages between the molecules and this crosslinking increased the rigidity of the PBE system [55]. These findings show good agreement our XRD observation and we conclude that the PZ6 was the most amorphous sample with the lowest T_g . Which in turn could give desirable conductivity properties.

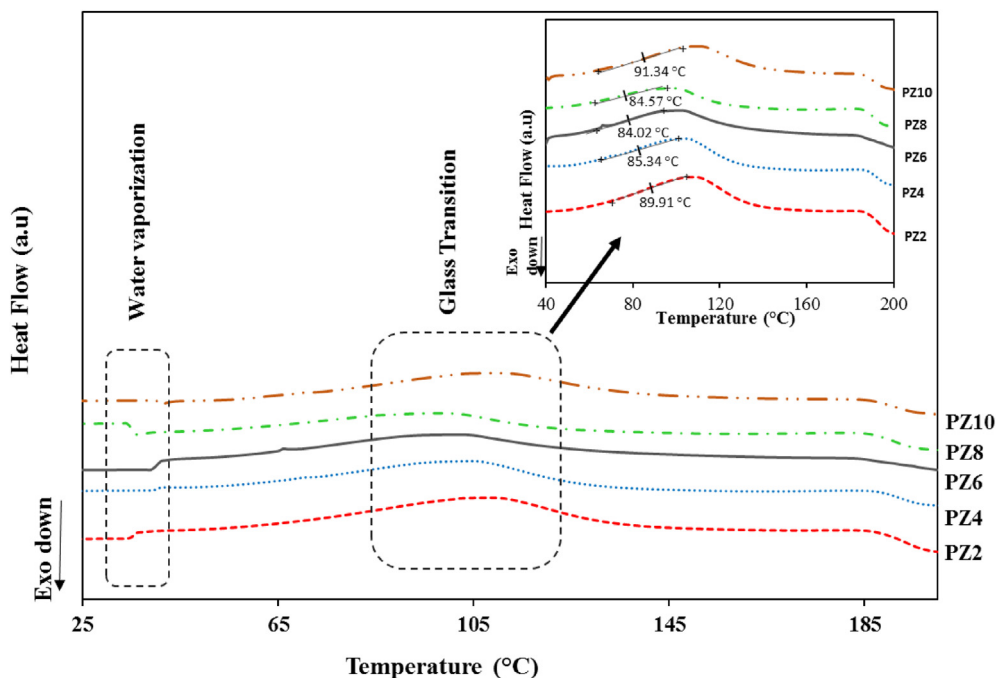


Fig. 4 – DSC thermogram for various content CMC–PVA –NH₄NO₃–EC.

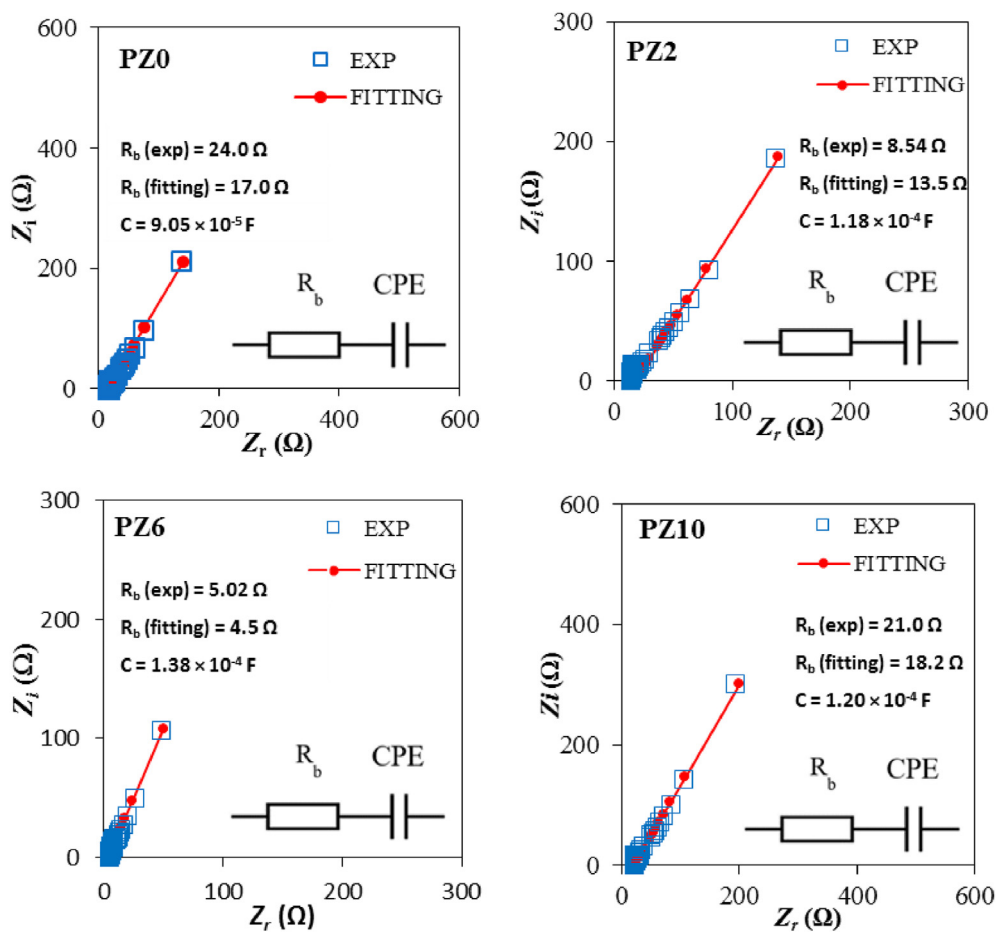


Fig. 5 – Nyquist plots and equivalent circuits of various contents of CMC–PVA–NH₄NO₃–EC.

Impedance analysis

Fig. 5 Shows the experimental and theoretical fitting of the Nyquist plot for various samples of the CMC–PVA–NH₄NO₃–EC. The Nyquist plots were represented by an inclined spike which indicated the presence of electrode polarization that are attributed to the diffusion process [56,57]. Furthermore, the disappearance of the semicircle may be due to the ruling effect of the resistive element of the polymer blend itself [58]. The inclined spike observed for all samples were fitted based on the theoretical equivalent circuit consisting of a series connection of R_b and CPE which adopted the following equation and presented as the inset in Fig. 5 including with the calculated parameter.

$$Z_r = R_b + \frac{k_2 \cos(\frac{\pi p_2}{2})}{\omega^{p_2}} \quad (4)$$

$$Z_i = \frac{k_2 \sin(\frac{\pi p_2}{2})}{\omega^{p_2}} \quad (5)$$

where R_b corresponds to the bulk resistance, k_2 is referring to the electrical double layer capacitance that occurred at the electrode/electrolyte interface during the measurement, ω is the angular frequency also equivalence to $2\pi f$, whereas p_2 is the skew parameter which controls the degree of the inclined spike from the Z_r axis. From the Nyquist plots, the values of parameters k_2 and p_2 were obtained by the fitting method until the fitted points gave a good fit to the experimental data [29].

Based on Fig. 5, the occurrence of tilted spike for all of the samples at the angle $\leq 90^\circ$ was ascribed to the inhomogeneous nature of the electrode-electrolyte interface [59]. Since the present work used stainless steel blocking electrodes for impedance analysis, the electrode-electrolyte interface can thus be regarded as a capacitance. As observed in the Nyquist plot, the addition of the EC caused the plot to move towards a higher frequency region and this was attributed to faster dipolar relaxation in the PBE which is supported by the increase in the degree of amorphous phase as discussed in XRD analysis previously.

As shown in Fig. 5, it's confirmed the reduction of R_b value from 24.0 Ω to 5.02 Ω when EC was introduced which reflects the increment of ionic conductivity. The reduction could be ascribed to three aspects which were predominant by the EC being the plasticizer. The first aspect is to provide a large free volume of comparatively excellent conducting phase [60]; the second aspect is to provide a better thermal stability to open up narrow rivulets of the plasticizer-rich phase in order to achieve superior ionic transport [61] and the third aspect is to increase the vibrational dynamic amplitude of host polymer which could enhance greater degree of salt dissociation to boost the ionic conductivity [62].

Ionic conductivity analysis

The ionic conductivity of various CMC–PVA–NH₄NO₃–EC samples obtained from the Nyquist plots were calculated and presented as ionic conductance plots in Fig. 6. In Fig. 6, there is a clear trend of increasing followed by a plateau region in the ionic conductivity trend. It is worth noting that the increasing trend in ionic conductivity with the increasing frequency is apparent at

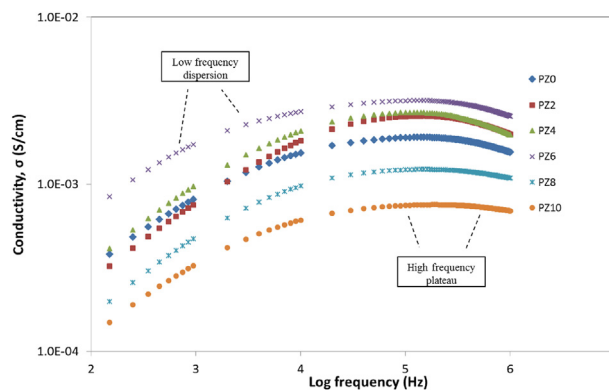


Fig. 6 – Ionic conductance plot of various contents of CMC–PVA–NH₄NO₃–EC.

low to medium frequency range which was attributed to the space charge polarization [63]. As the frequency increased, the number of free ions that was polarized also increased during the charge accumulation at the electrode-electrolyte interface. This trend seems to be consistent with those of previous studies [64,65]. The addition of EC is believed to be able to weaken the Coulombic force experienced by the cation and anion of the ionic dopant, thus releasing the ion of interest (H^+) more easily, hence increasing the ionic conductivity of CMC–PVA–NH₄NO₃–EC. As revealed by the XRD analysis, the incorporation of EC has been found to modify the degree of amorphousness which was ascribed to the complexation that has taken place between the EC and CMC–PVA–NH₄NO₃ which involved bond breakage and allowing the oxygen to be more occupied [18]. Thus, the oxygen became more susceptible to permit a large number of H^+ to migrate with less restriction via the flexible pathway and affect the conduction ability. It is also interesting to note that the addition of EC managed to decrease the glass transition (T_g) which increased the chain mobility and flexibility thus, facilitating the movement of ions which caused the ionic conductivity to increase as the EC content increased in this present system.

The most striking result to emerge from Fig. 6 is that the PZ6 sample with 6 wt % of EC had its ionic conductivity increased to $\sim 5.03 \times 10^{-3}$ S/cm when the frequency increased. This was sufficient to promote more dissociation of H^+ form quaternary ammonium ion via the vibration of the electric field into the sample when frequency was applied and thus, boost the ionic conductivity to a higher value. As a result, the maximum conductivity of PZ6 obtained was higher than the other samples and is comparable with the values reported in the literature [59,66,67]. This evaluation is aligned with the structural analysis observation, where PZ6 was the most amorphous sample and was able to provide more open channels for greater ionic transport conduction. Apparently, as the amorphous region increases, free volumes within the polymer electrolyte system increases as well which allows minimal restriction on the segmental motion of the polymer chain to favour the H^+ migration, resulting in higher ionic conductivity [61]. Mobile H^+ ions of tend to migrate more freely toward the active functional group, $-COO^-$ and enhance the formation of inter- and intra-molecular dipole-dipole forces and H-bonding as mentioned in the FTIR analysis.

However, ionic conductivity appeared to decrease with the addition of 8 and 10 wt % of EC and this can be ascribed to clogged in the polymer blend complexes where the dissociation of the ionic dopant was suppressed. This would cause a considerable amount of H^+ unable to be captured in the CMC–PVA– NH_4NO_3 system when EC was added, thus decreasing the ionic conductivity. Ng and Mohamad [68] reported that as the amount of plasticizers increased after reaching the maximum value in ionic conductivity, the host polymer matrix became overcrowded with ions including H^+ . Consequently, the transportation of charge carriers was reduced because of the limitation of ionic mobility [69].

The ionic conductivity of the CMC–PVA– NH_4NO_3 –EC at a range of various temperatures was also studied and depicted in Fig. 7. Based on Fig. 7(a), the ionic conductivity of the CMC–PVA– NH_4NO_3 –EC increased with increasing temperature. Heat exposure to the PBE causes the segmental motion to be thermally activated and possesses sufficient energy for the polymer chain to vibrate [70,71]. As the temperature increases, thermal movement of the PBE and dissociation of NH_4NO_3 become improved. The regression values (R^2) obtained from the temperature dependence plot was approaching ~1 which verified that all samples obey the Arrhenius behavior [72,73]. The Arrhenius behavior can be represented by the following equation:

$$\sigma = \sigma_0 \exp\left(-\frac{E_a}{kT}\right) \quad (6)$$

The absence of a sudden rise or drop in the ionic conductivity throughout the heating process proved that the ionic conductivity was predominantly due to the presence of the charge carrier (H^+) from the NH_4NO_3 which was enhanced with the addition of plasticizer, and was not affected by the solvent content. These findings are in agreement with those of Sim, Yahya [74] who also found that only the charge carrier is responsible in the conduction mechanism at the elevated temperatures.

The extension of this temperature study is the conductivity study for various compositions of EC at selected temperatures and presented in Fig. 7(b). A previous report has emphasized

that the temperature is crucial to correlate to the energy required by the ions to be dissociated and migrate from one site to another site throughout the conduction mechanism [75]. Fig. 7(b) shows that the trend in ionic conductivity is apparently in accordance to the conductance plot previously shown in Fig. 6. The highest conducting sample PZ6, showed the highest trend at higher temperatures. In this work, the addition of EC may affect the segmental motion of the PBE at higher temperatures which enhanced the bond rotation, thus resulting in faster H^+ migration from one vacant site to another via a new pathway as illustrated in Scheme 2 in the FTIR analysis. Overall, the net result demonstrated a progressive ionic conductivity improvement along with increasing temperature for all plasticized PBE. This behavior will promote the releasing and coordinating for rapid ions conduction.

Transport properties analysis

In this present work, transport properties including diffusion coefficient (D), ionic mobility (μ) and number of free mobile ions (η) were determined according to the procedure used by Arof and co-workers or also known as the Impedance Nyquist theoretical method (INT) where relevant impedance equations were used to derive the transport properties equation [29]. The equivalent circuit parameters which were determined from the Nyquist plot is very important to produce the relevant transport parameters equations including ionic mobility (μ), mobile ions (η), and diffusion coefficient (D). The information obtained from the Nyquist plot based on the fitting method are required to derive the following equations [29]:

$$\frac{\epsilon_r \epsilon_0 A}{t} = \frac{2k_2}{R_b^2 \omega_2^2} \quad (7)$$

$$D = (k_2 \epsilon_r \epsilon_0 A)^2 \omega_2 \quad (8)$$

Since the Nyquist plot presented in the previous section only consisted of spikes, the equation should be modified by

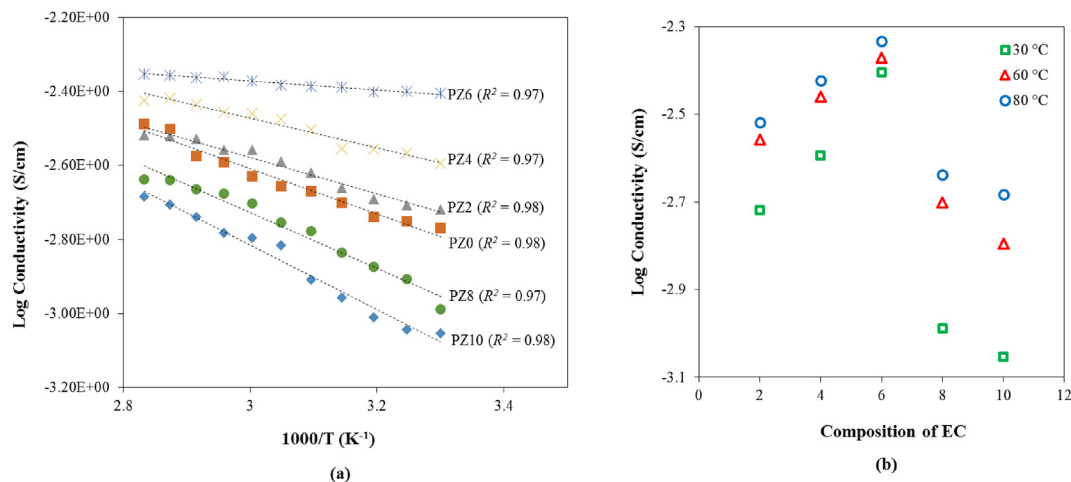


Fig. 7 – (a) Variation of conductivity with temperature dependence of various content of CMC–PVA– NH_4NO_3 –EC and (b) Conductivity for the CMC–PVA– NH_4NO_3 –EC at 30, 60 and 80 °C.

substituting equation (7) into equation (8), thus give the following equation (9) which is independent of ϵ_r value. Therefore, in this present work that involved spike system, diffusion coefficient (D_s) was determined using the following equation:

$$D_s = \frac{4k_2^4 t^2}{R_b^4 \omega_2^3} \quad (9)$$

Meanwhile, ionic mobility (μ) and mobile ions (η) were determined through the following:

$$\mu = \frac{eD_s}{k_b T} \quad (8a)$$

$$\eta = \frac{\sigma}{e\mu} \quad (9a)$$

where σ represents the ionic conductivity, k_b is the Boltzmann constant ($1.38 \times 10^{-23} \text{ J K}^{-1}$), T is room temperature in Kelvin (303 K), e is electric charge constant ($1.602 \times 10^{-19} \text{ C}$) and A is area of the sample. Fig. 8 provides the variation in transport parameters and ionic conductivity of various contents of EC.

Notably for this PBE system, the number of ions (η) was increased gradually as more EC was added into the CMC–PVA– NH_4NO_3 but it is in contrast to ionic mobility (μ) and ionic diffusion (D). The increment in η values were related to the increasing number of ionic species produced from the

dissociation of ionic dopant assisted by the plasticizer, EC. As seen in the figure, there was a significant correlation between the ionic conductivity of the PBE with the number of ions when 2 to 6 wt % of EC were added. This happened when sufficient amount of EC was added into the PBE which possibly provided more space for the ion transport with concomitant increases in ionic mobility (μ), ionic diffusion (D) and hence the ionic conductivity. Furthermore, the sample has greater tendency to become more amorphous and allowed the free mobile ions to move more easily as evidenced by the XRD analysis. This allows the free ions to complex with the PBE which in turn increased the ionic conductivity and ionic transport properties until the highest conductivity was obtained. As shown in Fig. 8, PZ6 achieved the highest ionic conductivity with the content of 6 wt % EC. Interestingly, the η value kept increasing even when the ionic conductivity decreased after the addition of EC beyond 6 wt %. Again, this trend corroborates the fact that the addition of EC has weakened the Coulombic forces in the ionic dopant and promoted further dissociation of ion pairs or aggregates of the NH_4NO_3 which caused the η to keep increasing.

Nonetheless, sample PZ8 and PZ10 demonstrated a decreasing trend in the ion diffusion and mobility, which suggested that excessive EC content (above 6 wt %) might cause blockages in the pathway during the H^+ migration process from NH_4NO_3 and hence, reducing the ionic mobility

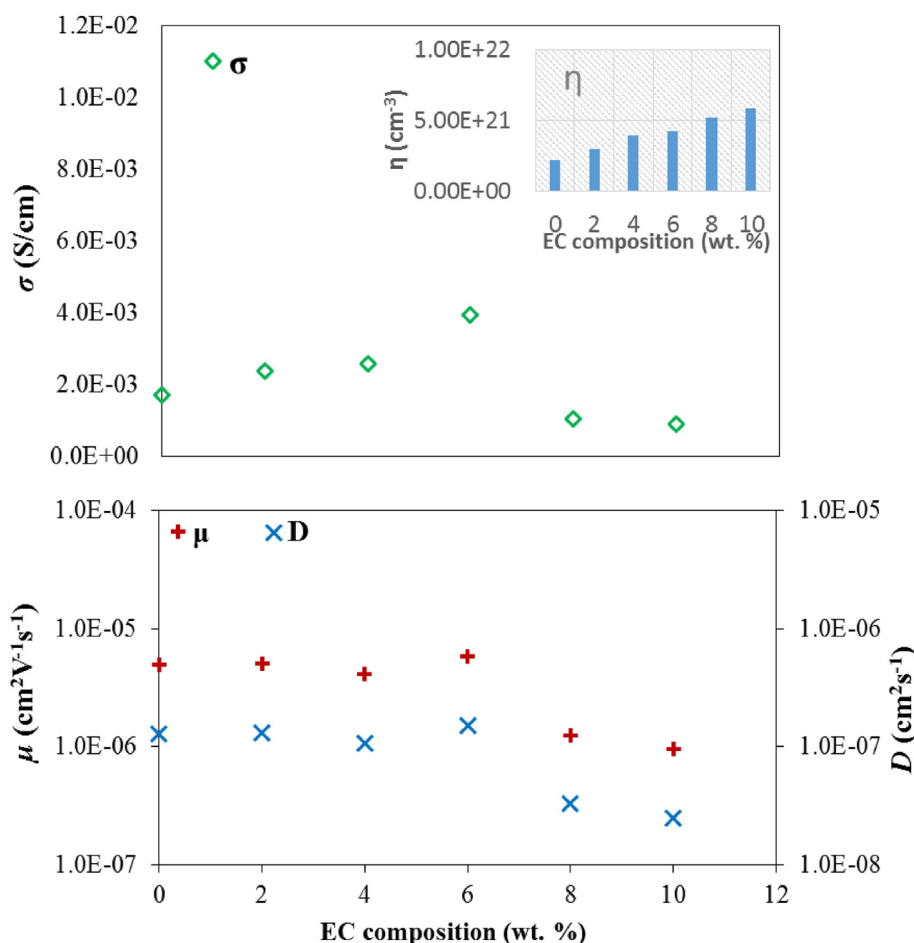


Fig. 8 – Variation in the ionic transport parameters of the CMC–PVA– NH_4NO_3 –EC system.

and also ions diffusion. In addition, the DSC analysis also revealed the increment in T_g for PZ8 and PZ10 that indicated these samples might experience the effect of pseudo cross-linking and caused the samples to become rigid and hence limit the ion diffusion and mobility which eventually decreased the ionic conductivity [76]. These results are supported by the fact that the ionic conductivity was governed by the ionic mobility (μ) and ionic diffusion (D) instead of the number of ions (η). It was observed that even if the number of ions was increasing, the ionic conductivity still decreased and this may be due to the higher number of ions having a higher probability of forming ion clusters which can restrict the ion mobility and ion diffusion. This phenomenon was also supported by other researchers [77,78].

Proton transference analysis

Determination of proton transference number measurement of the PZ6 sample which was the best CMC–PVA–NH₄NO₃–EC PBE system was performed using Bruce and Vincent's technique [79]. The incorporation of EC into the PBE system showed a remarkable effect where the ionic conductivity was increased due to the optimum plasticizer content. Obviously, this will affect the total current involved and generated. The PZ6 sample was sandwiched between MnO₂ electrodes as shown in Fig. 9 (a).

Manganese was selected to serve as the non-blocking electrode since the mobile ions that are expected to be present in this PBE system are protons (H⁺). This electrode was employed for the transference measurement where protons can pass through it. Fig. 9(b) presents the Nyquist plot for the determination of initial resistance (R_o) and steady state resistance (R_{ss}) in PZ6 whereas the plot of polarization current is depicted as the inset in Fig. 9(b). It is essential to measure the

initial current (I_o) and steady state current from the polarization current plot where the I_o obtained was 3.1 μ A and become fully depleted at an I_{ss} of 1.6 μ A. Based on the polarization current plot, the initial total current underwent rapid decrement in a longer time period of 315 s compared to previous reported system (CMC–PVA–NH₄NO₃) that took about 145 s [16]. This indicated that number of ions had increased in the electrolyte and the remaining current was ascribed to the migration of electron [71].

On the other hand, the values of initial resistance (R_o) and steady state resistance (R_{ss}) were determined based on the complex impedance measurement using MnO₂ electrodes which are specialized to determine the H⁺ ion where the R_o and R_{ss} values obtained were 913 Ω and 1044 Ω , respectively. The information obtained was then used in the determination of cation transference number (t_{H^+}) which was measured as 0.48. The t_{H^+} value measured in the present system is much higher than the previous system (CMC–PVA–NH₄NO₃) with a value of 0.42 [16]. This can be supported by the releasing and coordinating process of H⁺ from the H⁺–NH₃ which was assisted by the addition of EC, which later increased the number of t_{H^+} . These findings are comparable to other works reported by Prajapati, Roshan [80] and Kadir, Majid [81]. Thus, they confirm the effect of plasticization by the EC that can enhance the process of protonation and boost the ionic conductivity behavior, indicating that the CMC–PVA–NH₄NO₃–EC is an excellent candidate for applications as proton conducting electrolytes and for use in electrochemical devices. From the findings, it is clear that the enhancement of protonation due to the plasticization is crucial in improving the structural and electrical properties of the PBE while high ionic conductivity is important in the practical use of energy storage devices such as proton battery and supercapacitor.

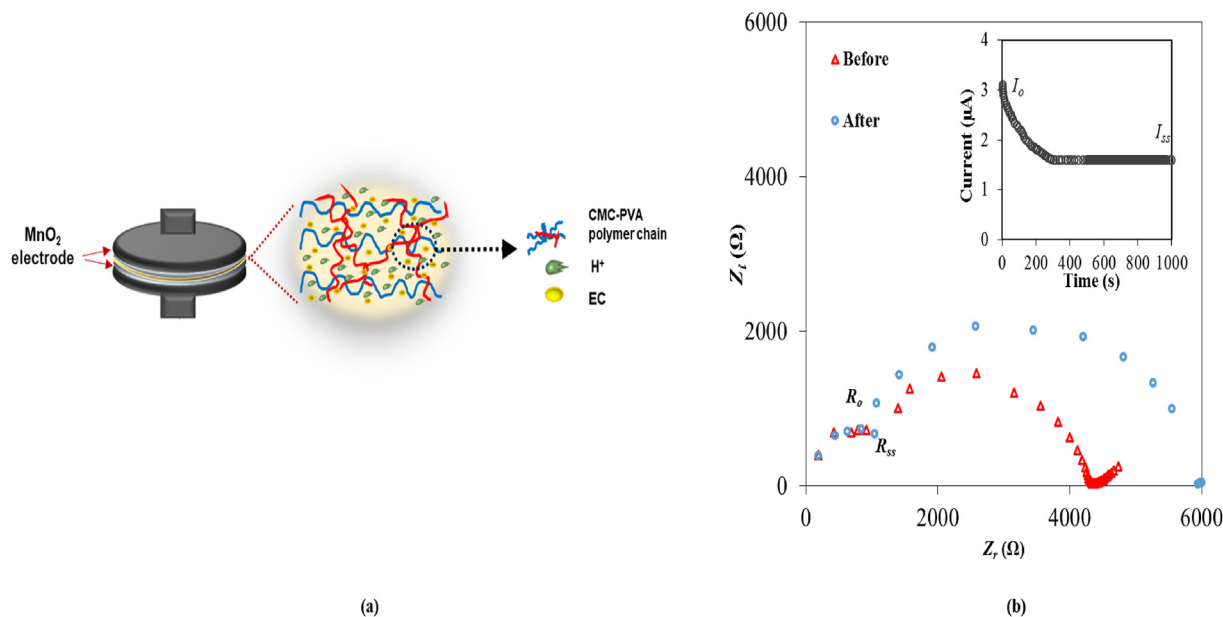


Fig. 9 – (a) Schematic diagram of H⁺ transference number measurement of PBE using manganese as non-blocking electrode and (b) Impedance plot for MnO₂/PZ6/MnO₂ cell at room temperature. Inset: Time dependence of polarization current for PZ6 at room temperature using non-blocking electrode.

Conclusion

A plasticized polymer blended electrolyte through CMC–PVA–NH₄NO₃ brings advances and novel properties in the solid state electrolyte system. The plasticization effect demonstrated by ethylene carbonate as a plasticizer was systematically characterized as intrinsically conducting polymers for its structural and ionic transport properties. The complexation of the PBE has affected the molecular properties and enhanced the miscibility region which in turn increased the degree of amorphous phase with optimum content of EC. The complexation between EC and NH₄NO₃ in assisting the dissociation of the ionic dopant, thereby inducing more ion-conducting phase region was highlighted at the conjugated π -system. The DSC analysis supported the miscibility of the entire system where the PZ6 sample was found to be the most amorphous sample, possessing the lowest T_g value during the glass transition phase. Based on the Impedance Nyquist theoretical (INT) approach, it was well supported that the ionic conductivity was mainly influenced by the ion transport D and μ , whereas the η kept increasing which was in alignment with the content of EC added. In the context of ionic conduction, proton was confirmed as the mobile charge carriers via the transference number measurement. Therefore, the structural and ionic transport upon the plasticization were confirmed by this present work where polymer blended electrolyte as highly potential substituent in order to expand the application of proton conducting polymer electrolytes in many electrochemical devices.

Declaration of competing interest

The authors declare that they have no known competing financial interests or personal relationships that could have appeared to influence the work reported in this paper.

Acknowledgement

The authors would like to thank the Ministry of Higher Education Malaysia (MOHE) for the FRGS grant (FRGS/1/2019/STG07/UMP/02/4) and Universiti Malaysia Pahang for the internal grant (RDU 190389) and postgraduate financial assistance (PGRS 190307), and finally the Faculty of Industrial Science & Technology, Universiti Malaysia Pahang for the technical and research support.

Appendix A. Supplementary data

Supplementary data to this article can be found online at <https://doi.org/10.1016/j.ijhydene.2021.02.187>.

REFERENCES

- [1] Fenton D. Complexes of alkali metal ions with poly (ethylene oxide). *Polymer* 1973;14:589.
- [2] Rahul, Bhattacharya B, Singh PK, Singh R, Khan ZH. Perovskite sensitized solar cell using solid polymer electrolyte. *Int J Hydrogen Energy* 2016;41:2847–52.
- [3] Yoon S, Ahmed F, Zhang W, Ryu T, Jin L, Kim D, et al. Flexible blend polymer electrolyte membranes with excellent conductivity for fuel cells. *Int J Hydrogen Energy* 2020;45:27611–21.
- [4] Li L, Wang F, Li J, Yang X, You J. Electrochemical performance of gel polymer electrolyte with ionic liquid and PUA/PMMA prepared by ultraviolet curing technology for lithium-ion battery. *Int J Hydrogen Energy* 2017;42:12087–93.
- [5] Zainuddin NK, Rasali NMJ, Mazuki NF, Saadiah MA, Samsudin AS. Investigation on favourable ionic conduction based on CMC-K carrageenan proton conducting hybrid solid bio-polymer electrolytes for applications in EDLC. *Int J Hydrogen Energy* 2020;45:8727–41.
- [6] Singh R, Singh PK, Singh V, Bhattacharya B. Quantitative analysis of ion transport mechanism in biopolymer electrolyte. *Optic Laser Technol* 2019;113:303–9.
- [7] Shakeel N, Ahamed MI, Ahmed A, Inamuddin Rahman MM, Asiri AM. Functionalized magnetic nanoparticle-reduced graphene oxide nanocomposite for enzymatic biofuel cell applications. *Int J Hydrogen Energy* 2019;44:28294–304.
- [8] Isa MIN, Sohaimy MIH, Ahmad NH. Carboxymethyl cellulose plasticized polymer application as bio-material in solid-state hydrogen ionic cell. *Int J Hydrogen Energy* 2021;46:8030–9.
- [9] Nadirah BN, Ong CC, Saheed MSM, Yusof YM, Shukur MF. Structural and conductivity studies of polyacrylonitrile/methylcellulose blend based electrolytes embedded with lithium iodide. *Int J Hydrogen Energy* 2020;45:19590–600.
- [10] Ben youcef H, Henkensmeier D, Balog S, Scherer GG, Gubler L. Copolymer synergistic coupling for chemical stability and improved gas barrier properties of a polymer electrolyte membrane for fuel cell applications. *Int J Hydrogen Energy* 2020;45:7059–68.
- [11] Majumdar S, Sen P, Ray R. Ionic interactions and transport properties in chitosan-starch based blend solid biopolymer electrolytes. *Mater Today: Proc* 2019;18:4913–20.
- [12] Liang YF, Xia Y, Zhang SZ, Wang XL, Xia XH, Gu CD, et al. A preeminent gel blending polymer electrolyte of poly(vinylidene fluoride-hexafluoropropylene)-poly(propylene carbonate) for solid-state lithium ion batteries. *Electrochim Acta* 2019;296:1064–9.
- [13] Thayumanasundaram S, Rangasamy VS, Seo JW, Locquet J-P. Electrochemical performance of polymer electrolytes based on Poly(vinyl alcohol)/Poly(acrylic acid) blend and Pyrrolidinium ionic liquid for lithium rechargeable batteries. *Electrochim Acta* 2017;240:371–8.
- [14] Sandoval C, Castro C, Gargallo L, Radic D, Freire J. Specific interactions in blends containing chitosan and functionalized polymers. *Molecular dynamics simulations. Polymer* 2005;46:10437–42.
- [15] Saadiah MA, Zhang D, Nagao Y, Muzakir SK, Samsudin AS. Reducing crystallinity on thin film based CMC/PVA hybrid polymer for application as a host in polymer electrolytes. *J Non-Cryst Solids* 2019;511:201–11.
- [16] Saadiah MA, Nagao Y, Samsudin AS. Proton (H⁺) transport properties of cmc-pva blended polymer solid electrolyte doped with NH₄NO₃. *Int J Hydrogen Energy* 2020;45:14880–96.
- [17] Gupta S, Varshney PK. Effect of plasticizer concentration on structural and electrical properties of hydroxyethyl cellulose (HEC)-based polymer electrolyte. *Ionics* 2017;23:1613–7.
- [18] Kumar R, Sharma S, Pathak D, Dhiman N, Arora N. Ionic conductivity, FTIR and thermal studies of nano-composite plasticized proton conducting polymer electrolytes. *Solid State Ionics* 2017;305:57–62.
- [19] Shin J, Jung S, Kim K, Ahn H, Ahn J. Preparation and characterization of plasticized polymer electrolytes based on

- the PVdF-HFP copolymer for lithium/sulfur battery. *J Mater Sci Mater Electron* 2002;13:727–33.
- [20] Richardson PM, Voice AM, Ward IM. Two distinct lithium diffusive species for polymer gel electrolytes containing LiBF₄, propylene carbonate (PC) and PVDF. *Int J Hydrogen Energy* 2014;39:2904–8.
- [21] Woo HJ, Majid SR, Arof AK. Effect of ethylene carbonate on proton conducting polymer electrolyte based on poly (ϵ -caprolactone)(PCL). *Solid State Ionics* 2013;252:102–8.
- [22] Chai MN, Isa MIN. Novel proton conducting solid biopolymer electrolytes based on carboxymethyl cellulose doped with oleic acid and plasticized with glycerol. *Sci Rep* 2016;6:27328.
- [23] Hamsan MH, Aziz SB, Azha MAS, Azli AA, Shukur MF, Yusof YM, et al. Solid-state double layer capacitors and protonic cell fabricated with dextran from *Leuconostoc mesenteroides* based green polymer electrolyte. *Mater Chem Phys* 2020;241:122290.
- [24] Shukur M, Ithnin R, Illias H, Kadir M. Proton conducting polymer electrolyte based on plasticized chitosan–PEO blend and application in electrochemical devices. *Opt Mater* 2013;35:1834–41.
- [25] Mishra K, Garg A, Sharma R, Gautam R, Pundir SS. Effect of blending of PMMA on PVdF-HFP + NaCF₃SO₃-EC-PC gel polymer electrolyte. *Mater Today: Proceedings* 2019;12:621–7.
- [26] Bandara TMWJ, Dissanayake MAKI, Albinsson I, Mellander B-E. Mobile charge carrier concentration and mobility of a polymer electrolyte containing PEO and Pr₄N⁺I⁻ using electrical and dielectric measurements. *Solid State Ionics* 2011;189:63–8.
- [27] Rice MJ, Roth WL. Ionic transport in super ionic conductors: a theoretical model. *J Solid State Chem* 1972;4:294–310.
- [28] Aziz SB, Karim WO, Brza M, Abdulwahid RT, Saeed SR, Al-Zangana S, et al. Ion transport study in CS: POZ based polymer membrane electrolytes using trukhan model. *Int J Mol Sci* 2019;20:5265.
- [29] Arof AK, Amirudin S, Yusof SZ, Noor IM. A method based on impedance spectroscopy to determine transport properties of polymer electrolytes. *Phys Chem Chem Phys* 2014;16:1856–67.
- [30] Vazhnova T, Lukyanov DB. Fourier self-deconvolution of the IR spectra as a tool for investigation of distinct functional groups in porous materials: brønsted acid sites in zeolites. *Anal Chem* 2013;85:11291–6.
- [31] Arof AK, Amirudin S, Yusof S, Noor IM. A method based on impedance spectroscopy to determine transport properties of polymer electrolytes. *Phys Chem Chem Phys : Phys Chem Chem Phys* 2013;16.
- [32] Aziz SB, B Marif R, Brza M, Hamsan M, Kadir M. Employing of trukhan model to estimate ion transport parameters in PVA based solid polymer electrolyte. *Polymers* 2019;11:1694.
- [33] Saadiah M, Samsudin A. Study on ionic conduction of solid biopolymer hybrid electrolytes based carboxymethyl cellulose (CMC)/polyvinyl alcohol (PVA) doped NH₄NO₃. *AIP Conf Proc: AIP Publishing* 2018:020223.
- [34] Saadiah M, Samsudin A. Electrical study on Carboxymethyl Cellulose-Polyvinyl alcohol based biopolymer blend electrolytes. *IOP Conference Series: Materials Science and Engineering: IOP Publishing*; 2018, 012045.
- [35] Watanabe M, Rikukawa M, Sanui K, Ogata N. Evaluation of ionic mobility and transference number in a polymeric solid electrolyte by isothermal transient ionic current method. *J Appl Phys* 1985;58:736–40.
- [36] Woo HJ, Majid SR, Arof AK. Transference number and structural analysis of proton conducting polymer electrolyte based on poly (ϵ -caprolactone). *Mater Res Innovat* 2011;15:49–54.
- [37] Sureshini AM, Nishimoto A, Watanabe M. Transport and electrochemical characterization of plasticized poly (vinyl chloride) solid electrolytes. *Solid State Ionics* 1996;86:385–93.
- [38] Wang P, Zhang H, Chai J, Liu T, Hu R, Zhang Z, et al. A novel single-ion conducting gel polymer electrolyte based on polymeric sodium tartaric acid borate for elevated-temperature sodium metal batteries. *Solid State Ionics* 2019;337:140–6.
- [39] Yusof Y, Shukur M, Hamsan M, Jumbri K, Kadir M. Plasticized solid polymer electrolyte based on natural polymer blend incorporated with lithium perchlorate for electrical double-layer capacitor fabrication. *Ionics* 2019;25:5473–84.
- [40] Ramli MA, Isa MIN. Structural and ionic transport properties of protonic conducting solid biopolymer electrolytes based on Carboxymethyl cellulose doped with ammonium fluoride. *J Phys Chem B* 2016;120:11567–73.
- [41] Altaf F, Gill R, Batool R, Drexler M, Alamgir F, Abbas G, et al. Proton conductivity and methanol permeability study of polymer electrolyte membranes with range of functionalized clay content for fuel cell application. *Eur Polym J* 2019;110:155–67.
- [42] Jiang H, Zhang Q, Zhang Y, Sui L, Wu G, Yuan K, et al. Li-Ion solvation in propylene carbonate electrolytes determined by molecular rotational measurements. *Phys Chem Chem Phys* 2019;21:10417–22.
- [43] Rahamathullah R, Khairul WM, Isa MIN. Contribution of stilbene-imine additives on the structural, ionic conductivity performance and theoretical evaluation on CMC-based biopolymer electrolytes. *Carbohydr Polym* 2020;250:116935.
- [44] Hafiza M, Isa M. Solid polymer electrolyte production from 2-hydroxyethyl cellulose: effect of ammonium nitrate composition on its structural properties. *Carbohydr Polym* 2017;165:123–31.
- [45] Hafiza MN, Isa MIN. Correlation between structural, ion transport and ionic conductivity of plasticized 2-hydroxyethyl cellulose based solid biopolymer electrolyte. *J Membr Sci* 2020;597:117176.
- [46] Perumal P, Christopher Selvin P, Selvasekarapandian S, Sivaraj P, Abhilash KP, Moniha V, et al. Plasticizer incorporated, novel eco-friendly bio-polymer based solid biopolymer membrane for electrochemical clean energy applications. *Polym Degrad Stabil* 2019;159:43–53.
- [47] Ravi M, Song S, Gu K, Tang J, Zhang Z. Electrical properties of biodegradable poly (ϵ -caprolactone): lithium thiocyanate complexed polymer electrolyte films. *Mater Sci Eng, B* 2015;195:74–83.
- [48] Ramya C, Selvasekarapandian S, Hirankumar G, Savitha T, Angelo P. Investigation on dielectric relaxations of PVP–NH₄SCN polymer electrolyte. *J Non-Cryst Solids* 2008;354:1494–502.
- [49] Liew C-W, Ramesh S. Electrical, structural, thermal and electrochemical properties of corn starch-based biopolymer electrolytes. *Carbohydr Polym* 2015;124:222–8.
- [50] Devi GN, Chitra S, Selvasekarapandian S, Premalatha M, Monisha S, Saranya J. Synthesis and characterization of dextrin-based polymer electrolytes for potential applications in energy storage devices. *Ionics* 2017;23:3377–88.
- [51] Latha C, Venkatachalam K. Synthesis and characterization of PVP: PVC: NH₄NO₃. *J Pure Appl Ind Phys* 2016;6:199–206.
- [52] Cassu SN, Felisberti MI. Poly (vinyl alcohol) and poly (vinyl pyrrolidone) blends: miscibility, microheterogeneity and free volume change. *Polymer* 1997;38:3907–11.
- [53] Klähn M, Krishnan R, Phang JM, Lim FCH, van Herk AM, Jana S. Effect of external and internal plasticization on the glass transition temperature of (Meth)acrylate polymers studied with molecular dynamics simulations and calorimetry. *Polymer* 2019;179:121635.

- [54] Dixon D, Ford M, Mantell G. Thermal stabilization of poly (alkylene carbonate) s. *J Polym Sci, Polym Lett Ed* 1980;18:131–4.
- [55] Noor NAM, Isa MIN. Investigation on transport and thermal studies of solid polymer electrolyte based on carboxymethyl cellulose doped ammonium thiocyanate for potential application in electrochemical devices. *Int J Hydrogen Energy* 2019;44:8298–306.
- [56] Shukur MF, Kadir MFZ. Electrical and transport properties of NH₄Br-doped cornstarch-based solid biopolymer electrolyte. *Ionics* 2015;21:111–24.
- [57] Samsudin A, Isa M. Structural and ionic transport study on CMC doped NH₄Br: a new types of biopolymer electrolytes. *J Appl Sci* 2012;12:174–9.
- [58] Hema M, Selvasekerapandian S, Sakunthala A, Arunkumar D, Nithya H. Structural, vibrational and electrical characterization of PVA–NH₄Br polymer electrolyte system. *Phys B Condens Matter* 2008;403:2740–7.
- [59] Rasali NMJ, Samsudin AS. Ionic transport properties of protonic conducting solid biopolymer electrolytes based on enhanced carboxymethyl cellulose - NH₄Br with glycerol. *Ionics* 2018;24:1639–50.
- [60] Isa M, Samsudin A. Ionic conduction behavior of CMC based green polymer electrolytes. *Advanced Materials Research: Trans Tech Publ*; 2013. p. 194–8.
- [61] Samsudin AS, Saadiah MA. Ionic conduction study of enhanced amorphous solid bio-polymer electrolytes based carboxymethyl cellulose doped NH₄Br. *J Non-Cryst Solids* 2018;497:19–29.
- [62] Aziz SB, Woo TJ, Kadir M, Ahmed HM. A conceptual review on polymer electrolytes and ion transport models. *J Sci: Adv Mater Dev* 2018;3:1–17.
- [63] Ramesh S, Ling OP. Effect of ethylene carbonate on the ionic conduction in poly (vinylidene fluoride-hexafluoropropylene) based solid polymer electrolytes. *Polym Chem* 2010;1:702–7.
- [64] Siekierski M, Wiczorek W, Przytuski J. AC conductivity studies of composite polymeric electrolytes. *Electrochim Acta* 1998;43:1339–42.
- [65] Tamilselvi P, Hema M. Conductivity studies of LiCF₃SO₃ doped PVA: PVdF blend polymer electrolyte. *Phys B Condens Matter* 2014;437:53–7.
- [66] Dhatarwal P, Sengwa RJ. Dielectric relaxation, Li-ion transport, electrochemical, and structural behaviour of PEO/PVDF/LiClO₄/TiO₂/PC-based plasticized nanocomposite solid polymer electrolyte films. *Compos Commun* 2020;17:182–91.
- [67] Sampathkumar L, Selvin PC, Selvasekarapandian S, Perumal P, Chitra R, Muthukrishnan M. Synthesis and characterization of biopolymer electrolyte based on tamarind seed polysaccharide, lithium perchlorate and ethylene carbonate for electrochemical applications. *Ionics* 2019;25:1067–82.
- [68] Ng L, Mohamad A. Protonic battery based on a plasticized chitosan-NH₄NO₃ solid polymer electrolyte. *J Power Sources* 2006;163:382–5.
- [69] Rozali M, Samsudin A, Isa M. Ion conducting mechanism of carboxy methylcellulose doped with ionic dopant salicylic acid based solid polymer electrolytes. *Int J Appl* 2012;2:113–21.
- [70] Aziz SB, Abidin ZHZ. Electrical conduction mechanism in solid polymer electrolytes: new concepts to arrhenius equation. *J Soft Matter* 2013;2013.
- [71] Moniha V, Alagar M, Selvasekarapandian S, Sundaresan B, Hemalatha R, Boopathi G. Synthesis and characterization of bio-polymer electrolyte based on iota-carrageenan with ammonium thiocyanate and its applications. *J Solid State Electrochem* 2018;22:3209–23.
- [72] Monisha S, Mathavan T, Selvasekarapandian S, Milton Franklin Benial A, Aristatil G, Mani N, et al. Investigation of bio polymer electrolyte based on cellulose acetate-ammonium nitrate for potential use in electrochemical devices. *Carbohydr Polym* 2017;157:38–47.
- [73] Rasali N, Nagao Y, Samsudin A. Enhancement on amorphous phase in solid biopolymer electrolyte based alginate doped NH₄NO₃. *Ionics* 2019;25:641–54.
- [74] Sim L, Yahya R, Arof A. Blend polymer electrolyte films based on poly (ethyl methacrylate)/poly (vinylidene fluoride-co-hexafluoropropylene) incorporated with 1-butyl-3-methyl imidazolium iodide ionic liquid. *Solid State Ionics* 2016;291:26–32.
- [75] Sohaimy M, Isa M. Ionic conductivity and conduction mechanism studies on cellulose based solid polymer electrolytes doped with ammonium carbonate. *Polym Bull* 2017;74:1371–86.
- [76] Noor I, Majid S, Arof A. Poly (vinyl alcohol)–LiBOB complexes for lithium–air cells. *Electrochim Acta* 2013;102:149–60.
- [77] Ahmed HT, Abdullah OG. Impedance and ionic transport properties of proton-conducting electrolytes based on polyethylene oxide/methylcellulose blend polymers. *J Sci: Adv Mater Dev* 2020;5:125–33.
- [78] Siddaiah T, Ojha P, Gopal NO, Ramu C, Nagabhushana H. Thermal, structural, optical and electrical properties of PVA/MAA:EA polymer blend filled with different concentrations of Lithium Perchlorate. *J Sci: Adv Mater Dev* 2018;3:456–63.
- [79] Bruce PG, Evans J, Vincent CA. Conductivity and transference number measurements on polymer electrolytes. *Solid State Ionics* 1988;28:918–22.
- [80] Prajapati G, Roshan R, Gupta P. Effect of plasticizer on ionic transport and dielectric properties of PVA–H₃PO₄ proton conducting polymeric electrolytes. *J Phys Chem Solid* 2010;71:1717–23.
- [81] Kadir M, Majid S, Arof A. Plasticized chitosan–PVA blend polymer electrolyte based proton battery. *Electrochim Acta* 2010;55:1475–82.